Blue Avalanche Upconversion in Tm:ZBLAN Fibre

S.Guy, D.P.Shepherd*, M.F.Joubert, and B.Jacquier

Laboratoire de Physico-Chimie des Matériaux Luminescents

Université Claude Bernard Lyon I

Bâtiment 205, 43 boulevard du 11-11-1918,

Villeurbanne CEDEX, France

H.Poignant

CNET-LANNION

LAB / RIO / TSO

22301 LANNION Cedex, France

Abstract

We report the investigation of the photon avalanche effect in heavily doped Tm:ZBLAN fibre at room temperature. Pumping at 630nm to 650nm, which is not resonant with the ground state absorption, gives intense blue emissions at 450nm and 480nm. The time evolution of the absorption and emission show a slow decaying oscillation before steady state is reached.

*Permanent address - Optoelectronics Research Centre, University of Southampton, Highfield, Southampton, U.K.

1. INTRODUCTION

There is currently a great interest in finding compact visible lasers for many applications and specifically in blue laser sources for increased storage density on optically written disks. Thulium doped ZBLAN fibre lasers have much promise in fulfilling this requirement with continuous blue upconversion laser action having been demonstrated at room temperature by Grubb *et al.*[1], by Barber *et al.*[2], and by Le Flohic *et al.*[3] . In the two former reports, three successive absorptions of pump photons in the 1100nm to 1180nm region are used to obtain an excited ion in the $^1G_4$ level. Laser action to the $^3H_6$ ground state can then occur at 480nm in low-doped ZBLAN fibre. In the third experiment two excitation wavelengths (645nm and 1064nm) are used to achieve laser action from the $^1D_2$ upper state to $^3F_4$ at 455nm. Here we investigate the behaviour of an alternative pumping scheme where the pump wavelength is resonant with an excited state absorption and not with the ground state absorption. Such an avalanche pumped laser has been demonstrated in Tm:$YLiF_4$[4] and gives new possible pumping wavelengths which may be more convenient than those found for ground state absorption. It also requires a different optimum doping level as higher concentrations are required to give the efficient cross-relaxations which are necessary in this pumping scheme. We report what we believe is the first observation of the avalanche effect in Tm:ZBLAN. A 3.2wt.% Tm doped ZBLAN fibre is pumped in the 630nm to 650nm range and the blue emission and excitation spectra, and a study of the time evolution of the fluorescence and absorption are given. A comparison is made to the results found by Oomen and Lous[5] for lightly doped Tm:ZBLAN glass.

2. PHOTON-AVALANCHE PUMPING

The avalanche effect may occur in the case where an efficient cross-relaxation energy-transfer leads to a build up of population in an excited-state from which a resonant absorption occurs to

a higher level. This effect has been modelled for a general 3-level case[6] and for the Tm system in particular[7,8] by Guy *et al.*. The energy level diagram for Tm showing the appropriate pumping scheme is shown in fig.1. The non-resonant absorption from the ground state populates the $^3F_2$ level which relaxes non-radiatively to the $^3H_4$ level. From here many possible excitation routes are possible including resonant excited state absorptions from $^3F_4$ to $^1G_4$ and $^3H_4$ to $^1D_2$, and several possible cross-relaxations which help to feed population into the $^3F_4$ level. The overall effect is to build up a large population in the long-lived $^3F_4$ level such that the pump absorption changes dramatically from an initially very low value to a very high value and that this effect occurs above a certain threshold pump power. The dominant radiative transitions give rise to fluorescence at 450nm ($^1D_2 \rightarrow {}^3F_4$) and 480nm ($^1G_4 \rightarrow {}^3H_6$).

3. EXPERIMENTAL DETAILS

Figure 2 shows the experimental apparatus used in these experiments. An argon-ion pumped dye laser (DCM or Kyton Red) was used as the pump source. After a beam collimator and chopper the light was launched with a X10 microscope objective into a 3.2 wt.% Tm doped ZBLAN fibre (grown by CNET). The fibre was cut to a length of 30cm corresponding to the point at which the blue fluorescence observed by eye from the side of the fibre had nearly died away. The light was coupled out of the fibre with another microscope objective and a beam splitter was used so that the pump transmission and the fluorescence could be observed simultaneously. The pump was focussed onto a silicon photodiode such that all the beam was collected and the fluorescence was observed through a half-meter focal length monochromator (from Jobin-Yvon) with a S-20 type photomultiplier (from EMI). The output signals were observed using a Lecroy 9410 oscilloscope.

A. Pump Power Dependance of Fluorescence Intensity and Pump Transmission

Two sets of measurements were taken corresponding to the two peak excitation wavelengths observed for the 480nm fluorescence. The pump power was varied and the corresponding transmitted pump intensity and fluorescence intensity were noted, as well as the time establishment of this upconverted fluorescence. The results are shown in fig.3(a) for 649nm and fig.3(b) for 633nm pumping. Both pump wavelengths exhibit an avalanche absorption behaviour but the 633nm pump gives more 480nm fluorescence (observed from the end of the fibre) and is less resonant with the ground state absorption (657nm)[9]. The values for pump transmission were calculated by assuming 100% transmission at very low pump power levels.

It can be seen that the fluorescence rise time, defined as the time necessary to reach stationary population of the emitting level, increases to a maximum value as the pump starts to show significant absorption. The rise times obtained (~100ms) are much larger than the normal fluorescence lifetimes of any of the levels shown in fig.1. The rise time reduces as the pump power is raised further and the absorption increases. The fluorescence power increases with the pump power (P) with a P^n dependance where n~2.2 for 649nm pumping and ~2.4 for 633nm pumping. Both show a reduction in the n factor for absorptions approaching 100%. It can also be seen that the threshold pump power required to achieve an avalanche effect is lower for 649nm pumping.

B. Pump Power Dependance of Fluorescence and Pump Temporal Profiles

Figures 4(a)-(h) show the temporal profile for the pump and fluorescence after the chopper opens, for several different pump powers at 649nm. At very low pump powers ((a), 0.09mW) we see no sign of a changing pump absorption with time. Increasing the power ((b) to (d), 0.18mW to 3mW) gives a lengthening of the fluorescence rise time and the pump profile starts to show increasing absorption with time. The rise time of the absorption mirrors that of the fluorescence.

By comparing figures 4(d),(e) and (f) it can be seen that the initial rise in the fluorescence changes from a convex shape to a straight line and finally to a concave shape. This is in agreement with the theoretical behaviour for the avalanche effect[10]. With further increases in power ((e) to (g), 6.7mW to 57mW) the fluorescence and absorption rise times become faster and the depth of the change in absorption increases. After 15mW of pump power the percentage difference between the initial transmission and the final 'cw' transmission no longer increases but measurements of the overall transmission show that it drops from 25% at 15mW (f) to around 2% at 217mW, (h). At high pump powers (>50mW) we begin to see an oscillation in the pump transmission before it reaches it's final 'cw' value. This feature has not previously been observed in avalanche processes. Figure 5(a) to (i) show the same thing for 633nm pumping which is further from the ground state resonant absorption. Similar effects are observed with the main differences being that the rise times can be longer in this case and the longest rise time occurs at a higher power. There is once again a very clear change from a convex to concave initial rise in fluorescence as seen in fig.5(d) and (e). The oscillating behaviour of the pump transmission (above 20mW) is much more pronounced in this case and it is clear that the fluorescence follows similar oscillations. It should be stressed that these oscillations are very stable from pulse to pulse. These oscillations have not been modelled but they must correspond to oscillations in the populations of the fluorescing ($^1G_4$) and absorbing ($^3F_4$, $^3H_4$) levels.

C. Fluorescence and Excitation Spectra

Fluorescence spectra were obtained with the apparatus shown in fig.2, using a computer to control the monochromator and to sample 100 points at each wavelength. On observing the fluorescence signal at the output of the fibre for different wavelengths it became clear that the spectra would depend on the particular part of the temporal profile that was sampled. At certain wavelengths (~450nm) an extraordinary short spike of ~1msec duration was observed as the

chopper opened (and typically stayed open for several hundred msec). For this reason a box car integrator was used which allowed us to gate either at the beginning of the excitation (where the peak occurs) or near the end (for the 'cw' spectrum). The monochromator slits were set to give a 1.2nm resolution. The fluorescence spectra obtained in this way will be significantly affected by absorption due to the long length of the sample. To eliminate absorption effects we also took spectra of the side-fluorescence. The fluorescence was collected near the beginning of the fibre with a 10cm focal length lens and then focussed into the same monochromator set up as described above except that no summations were taken for these spectra.

Excitation spectra were taken using similar apparatus except that this time the computer was used to control the dye laser wavelength. The spectra obtained are not corrected for the variation in the power of the dye laser but we checked that the general shape of the spectra were not too badly effected by carrying out excitation spectra with both a DCM and a Kyton Red dye which have opposite output power versus wavelength trends over the wavelength region in question.

i) Side-Fluorescence and Excitation Spectra

Figure 6(a) to (e) shows the side-fluorescence spectra for varying 649nm pump power. The position of the two blue emission peaks is in agreement with those found in optically thin, lightly doped samples by Oomen and Lous[5]. The band around 450nm is ascribed to the $^1D_2 \rightarrow {}^3F_4$ transition and that at 480nm is ascribed to the $^1G_4 \rightarrow {}^3H_6$ transition. It can be seen in figure 6 that the ratio of the intensity of the emissions varies with the pump power. At pump powers incident on the input objective of less than 65mW the 480nm band is larger whereas above this value the 450nm band dominates the spectrum. Thus the 450nm emission seems to have a more non-linear response to pump power than the 480nm emission. This is to be expected as a larger number of pump photons can be involved in excitation to the $^1D_2$ level than to the $^1G_4$ level (see

fig.1). The excitation spectra for the two emission bands are shown in fig.7. Both spectra are at a maximum around 649nm and a reduced maximum at 633nm is only observed for the fluorescence at 480nm. This is in contrast to the results for lightly doped samples where the 480nm band is at a maximum for ~649nm but the 450nm band is at a maximum for ~657nm pumping (corresponding to a ground state absorption[9]).

In lightly-doped ZBLAN bulk material where photon avalanche does not occur, $^1D_2$ is populated by sequential absorption of two photons. On the contrary, in heavily-doped ZBLAN fibre, $^1D_2$ is more efficiently populated via photon avalanche. This point will be more developed later.

ii) End-Fluorescence and Excitation Spectra

The excitation spectra for the two blue emmision bands for fluorescence collected from the end of the fibre are shown in fig. 8. The main difference to those observed from the side is that, now, the most efficient excitation for the 480nm fluorescence is centered around 633nm (fig. 8a). This peak is not observed in the lightly doped samples [5,9] and must be due to the excited state absorption $^3F_4 \rightarrow {}^1G_4$ characteristic of the photon avalanche effect.

The end collected fluorescence spectra for pumping at the two excitation peaks given in figure 8(a) are shown in fig.9(a) to (d) for different pump powers and sampling different parts of the temporal profile. Fig. 9 (a) and (b) take the case of 649nm excitation. The solid lines are the spectra found when gating a long time after the chopper opens on the 'cw' part of the temporal profile. The 480nm emission band is now at a maximum at around 485nm and the 450nm band is now at a maximum at around 455nm. These spectra are consistent with these emission bands suffering from a large absorption on their short wavelength side. In the case of the 480nm band this is due to ground state absorption $^3H_6 \rightarrow {}^1G_4$, whereas for the 450nm band this would be due to an excited state absorption $^3F_4 \rightarrow {}^1D_2$. The dashed line in fig. 9(a) and (b) is the spectra

obtained when sampling around 1ms after the onset of excitation. This is dominated by a peak at around 450nm which is in agreement with the peak position found from the side fluorescence measurements. The other band is still peaked at around 485nm. This is consistent with the fact that the 480nm band is always affected by ground state absorption, whereas the 450nm band is not affected until the avalanche process has had time to build up a significant population in an excited state (the long lived $^3F_4$ level) which then causes absorption of these wavelengths. This is also consistent with the observed gradual shifting to lower wavelengths of the peak of the 450nm band to lower wavelengths with lower pump power.

Fig 9(a) also shows a significant green fluorescence. This can be attributed to the $^1D_2 \rightarrow {}^3H_5$ transition[9] and appears to be so strong in the high power 'cw' spectra due to the fact that it is the only line shown that does not suffer from a large absorption effect. It's real significance is shown in the side-fluorescence measurements. The excitation spectra for the green emission is indistinguishable from that for the 450nm emission band as expected if they come from the same upper level.

The wavelength (450nm) at which just a short lived spike of fluorescence is observed corresponds to that on the spectra where the solid 'cw' line goes to zero while the dashed 'spike' line is near its maximum. The excitation spectra for the 'spike' was found by setting the monochromator to the appropriate wavelength (around 450nm) and sampling only the early part of the temporal profile. The result is shown in fig.8(d). The first thing that can be noted is that a small side peak in the excitation spectra can be observed at around 657nm. This corresponds to a ground state absorption feature[5,9] already mentioned, indicating that at this early stage of excitation the avalanche process has not had enough time to build up significant excited state populations and so the ground state absorption is more important. However the peak of the excitation spectra occurs at around 642nm. We propose to assign this 642nm band to the excited state absorption $^3H_4 \rightarrow {}^1D_2$. Indeed, at short time in the avalanche regime, the 450nm maximum

fluorescence obtained from the 649nm excitation is mostly radiatively trapped and does not contribute to the output signal while the 643nm absorption, which is not efficient for avalanche, gives a better excitation channel for the $^1D_2$ fluorescence measured at the output of the fibre. As the population of the $^3F_4$ is built (`cw' regime), the 642nm absorption is less probable than the avalanche mechanism. It should be noted that the contribution of the `pure' two-step excitation ($^3H_6 \rightarrow {}^3F_2$ and $^3H_4 \rightarrow {}^1D_2$) which dominates the initial excitation is weak compared to the avalanche mechanism which dominates the `cw' regime. The observation of oscillation in the fluorescence and absorption signals can be related to the reabsorption process, as a result of oscillation in the $^3F_4$ population. These oscillations are not observed in the side light measurements because no reabsorption is taken into account in that configuration.

D. Fluorescence Spatial Distribution

We were unable to observe a spatial modulation of the fluorescence intensity along the fibre as has previously been observed in avalanche pumped Er:ZBLAN fibre[11] and avalanche pumped Tm:YAG epitaxial waveguides[10]. It is possible that the blue fluorescence was so intense that we would have been unable to see the pattern even if it were present.

4 DISCUSSION

We have clearly pionted out that blue upconversion in a thulium-doped ZBLAN fibre is obtained by an avalanche mechanism via two excitation wavelengths, 649nm and 633nm, which are attributed to $^3F_4 \rightarrow {}^1G_4$ excited state absorption transitions. These two wavelengths are probably related to two crystal field components of the $^1G_4$ level as it is generally observed in other materials[4,7,8]. They also provide an excitation channel for an intense 450nm fluorescence.

In agreement with Oomen[5,9] we have observed the ground state absorption transition

attributed to $^3H_6 \rightarrow {}^3F_2$. Furthermore, we have detected a new absorption band at 642nm which has been attributed to the $^3H_4 \rightarrow {}^1D_2$ excited state absorption transition. Oomen et al could not detect this new excited state absorption in their lightly-doped material because the heavily-doped sample (3%) allows a noticable $^3H_4$ population in the early stage of the avalanche mechanism.

All these assignments correspond to an energy level diagram slightly different from that observed in the BIGaZYTZn:Tm glass where the avalanche wavelengths ($^3F_4 \rightarrow {}^1G_4$) are at shorter wavelengths than the $^3H_4 \rightarrow {}^1D_2$ excited state absorption transition[12]. In this case the overlap between ground state absorption and excited state absorption (from $^3H_4$ and $^3F_4$) transitions obscure the situation and contribute to the selectiveness of the excitation mechanism. At the same time, it provides a possible usefull channel for a strong 450nm fluorescence signal.

It is also interesting to consider the different crystal field behaviour encountered in two fluoride glasses characteristic of the beginning (ZBLAN) and the end (BIGaZYTZn) of the rare earth series.

4. CONCLUSION

Avalanche upconversion has been observed and characterised in a heavily doped Tm:ZBLAN fibre. An absorption of around 90% could be obtained in a 30cm length of fibre for 192mW of incident pump power at a wavelength of 633nm. This is a wavelength which is well removed from the resonant ground state absorption and which at low powers or in low doped samples has negligible absorption. Thus the avalanche pumping scheme can offer new possible pump wavelengths for this important laser system. Besides the normal increase in fluorescence rise time observed at avalanche threshold we have also observed an oscillatory behaviour in both the fluorescence and pump absorption above the threshold that gradually decays to a steady state value.

A power dependance of the ratio of 450nm to 480nm fluorescence has been demonstrated

and the end collected fluorescence have shown significant effects due to ground and excited state absorptions. The excitation spectra clearly show a different behaviour to those found in low doped samples with the most striking difference being a large broad excitation peak around 633nm for the 480nm emission.

It would be interesting to test whether laser action can be achieved by this pumping scheme and to compare the performance to the three-photon pumping scheme which is the only successful scheme for a one-wavelength-pumped Tm:ZBLAN blue upconversion laser system so far reported. It would be necessary to find the optimum Tm concentration which should be high enough to give efficient cross-relaxation processes but not so high that there is a strong quenching of the upper laser level lifetime or a large increase in background propagation loss. It is also possible that other convenient pump wavelengths which are not resonant with the ground state absorption but with some excited state absorption may be found which also give efficient avalanche pumping of the appropriate levels. For instance from the results of ref.13 it would seem that 1.064μm pumping of Tm doped silica fibres has already been demonstrated to give an avalanche effect.

Acknowledgements

One of us (D.Shepherd) wishes to thank the Univesity of Lyon 1 for supporting his research during his saty at the laboratoire de Physico-Chimie des Materiaux Luminescents.

References

1. S. G. Grubb, K. W. Bennett, R. S. Cannon, and W. F. Humer, "Cw room-temperature blue upconversion fibre laser," Electron. Lett. **28**, 1243-1244 (1992).

2. P. R. Barber, C. J. Mackechnie, R. D. T. Lauder, H. M. Pask, A. C. Tropper, D. C. Hanna, S. D. Butterworth, M. J. McCarthy, J. -L. Archambault, and L. Reekie, "All solis state blue room temperature thulium-doped upconversion fiber laser," in *Compact Blue-Green Lasers*, Vol. 1 of 1994 OSA Technical Digest Series (Optical Society of America, Washington, D.C., 1994), paper CFA3.

3. M. P. Le Flohic, J. Y. Allain, G. M. Stéphan, and G. Mazé, "Room-temperature continuous-wave upconversion laser at 455nm in a Tm^{3+} fluorozirconate fiber," Opt. Lett. **19**, 1982-1984 (1994).

4. T. Herbert, R. Wannemacher, R. M. Macfarlane, and W. Lenth, "Blue continuously pumped upconversion lasing in Tm:YLF_4," Appl. Phys. Lett. **60**, 2592-2594 (1992).

5. E. W. J. L. Oomen and E. J. Lous, "A material and device study for obtaining a blue upconversion fibre laser," Philips J. Res. **46**, 157-198 (1992).

6. M. F. Joubert, S. Guy, and B. Jaquier, "Model of the photon-avalanche effect," Phys. Rev. B **48**, 10031-10037 (1993).

7. S. Guy, M. F. Joubert, B. Jacquier, and C. Linarès, "Blue avalanche upconversion in YAG:Tm," Radiation Effects and Defects in Solids **133-134**, (1995).

8. S. Guy, M. F. Joubert, and B. Jacquier, "Blue upconverted fluorescence via photon-avalanche pumping in YAG:Tm," Phys. Stat. Sol. (b) **183**, K33-K36 (1994).

9. E. W. J. L. Oomen, J. Non-Cryst. Solids **140**, 150-152 (1992), and E. W. J. L. Oomen, "Up-conversion of red light into blue light in thulium doped fluorozirconate glasses," J. Lumin. **50**, 317-332 (1992).

10. S. Guy, PhD Thesis (Lyon, Dec. 1995), "L'avalanche de photons : Application à l'ion Tm^{3+} dans differents materiaux".

11. Y. Chen and F. Auzel, "Spatial domains in avalanche pumped Er:ZBLAN fibre," Electr. Lett. **30**, 323-324 (1994).

12. M. F. Joubert, S. Guy, C.Linarès, B. Jacquier, J. L. Adam, "Avalanche upconversion in Tm^{3+}-doped BIGaZYTZn glass," J. Non-Cryst. Solids **184**, 98-102 (1995).

13. D. C. Hanna, R. M. Percival, I. R. Perry, R. G. Smart, J. E. Townsend, and A. C. Tropper, "Frequency upconversion in Tm- and Yb:Tm-doped silica fibers," Opt. Comm. **78**, 187-194 (1990).

Figure Captions

Fig. 1 Energy level diagram for Tm:ZBLAN showing the avalanche pumping scheme.

Fig.2 Experimental apparatus.

Fig.3 Graphs of 480nm fluorescence intensity, fluorescence rise time, and pump transmission, versus pump power for 649nm (a) and 633nm (b) pumping, observed from the end of the fibre.

Fig.4 Pump and fluorescence temporal profile for 649nm pumping at (a) 0.093mW, (b) 0.18mW, (c) 1.8mW, (d) 3mW, (e) 6.7mW, (f) 15mW, (g) 57mW, (h) 217mW, observed from the end of the fibre.

Fig.5 Pump and fluorescence temporal profile for 633nm pumping at (a) 0.9mW, (b) 1.8mW, (c) 3.3mW, (d) 6.5mW, (e) 20mW, (f) 31mW, (g) 60mW, (h) 122mW, (i) 224mW, observed from the end of the fibre.

Fig.6 Side-observed fluorescence spectra for 649nm pumping at (a) 118mW, (b) 36mW, (c) 10mW.

Fig.7 Side-observed excitation spectra for the 478nm (a) and 454nm (b) fluorescence.

Fig.8 End-observed excitation spectra for the 484nm (a), 459nm (b), and 513nm (c) fluorescences. (d) is the excitation spectrum of the 450nm 'spike' fluorescence.

Fig.9 End-observed fluorescence spectra for 649nm pumping at (a) 47mW and (b) 12mW, and for 633nm pumping at (c) 164mW and (d) 10mW. The dotted lines are the spectra sampled shortly after the onset of excitation and the solid lines are the spectra observed in the steady-state.

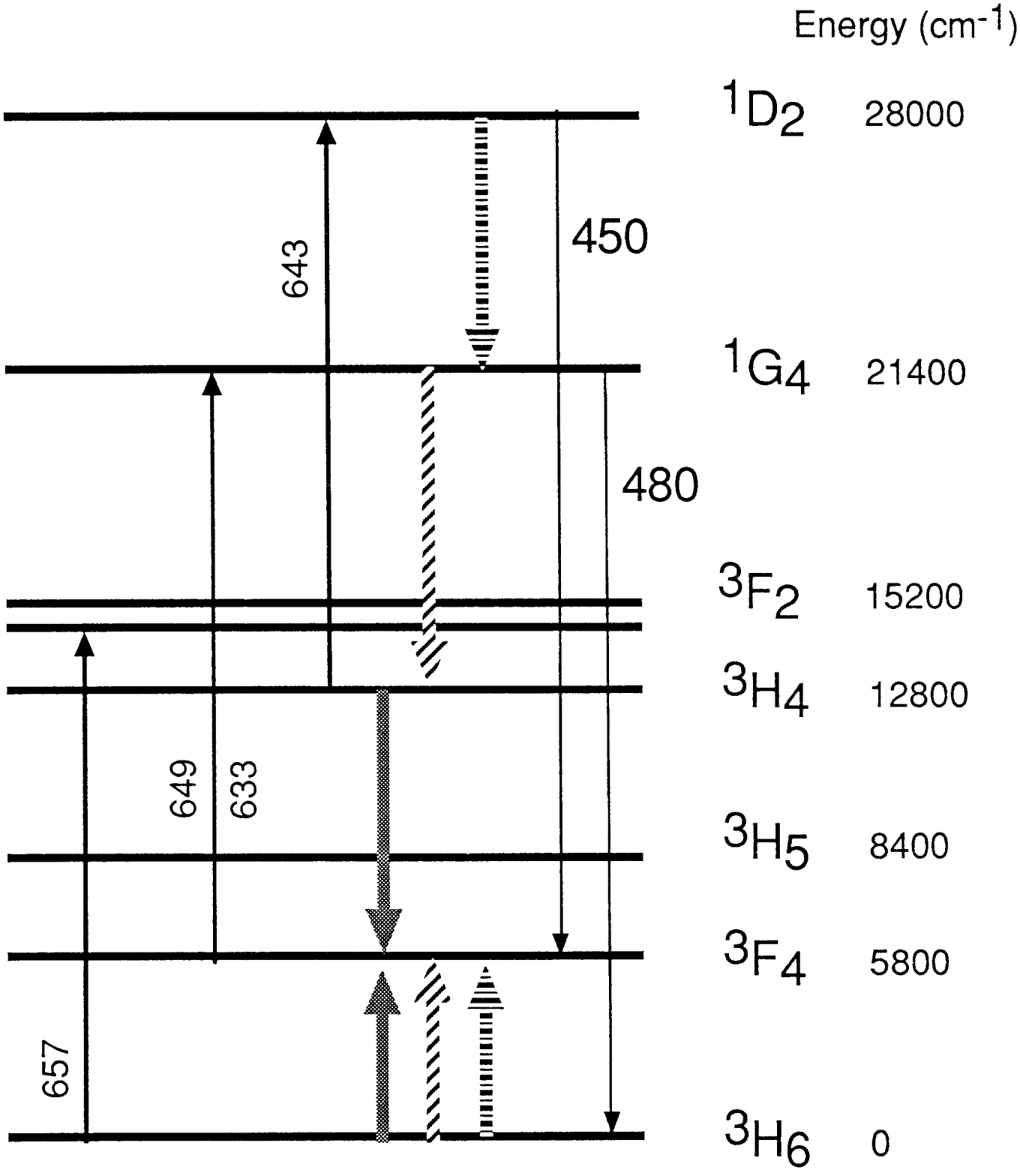
Energy (cm-1)
1D2
28000
1G4
21400
3F2
15200
3H4
12800
3H5
8400
3F4
5800
3H6
0
643
450
480
649
633
657

Fig 2

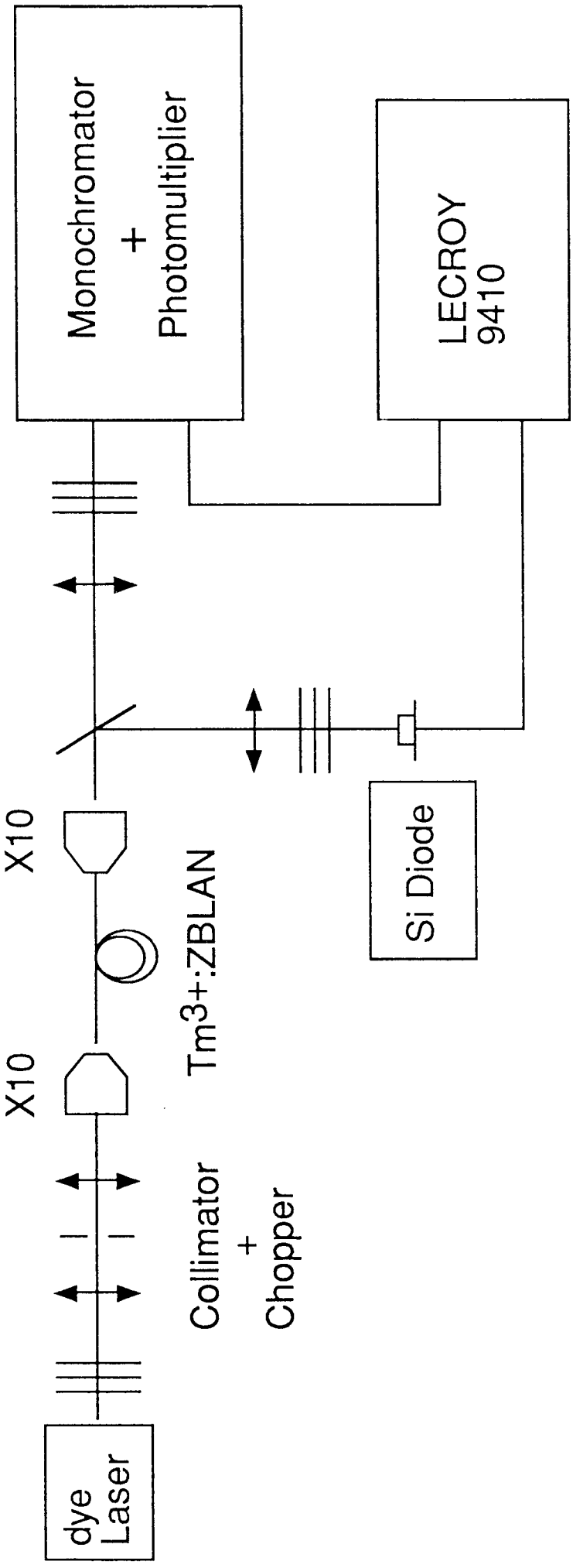
Monochromator
+
Photomultiplier
LECROY
9410
Si Diode
X10
X10
Tm^{3+}:ZBLAN
Collimator
+
Chopper
dye
Laser

Fig 5.

a)

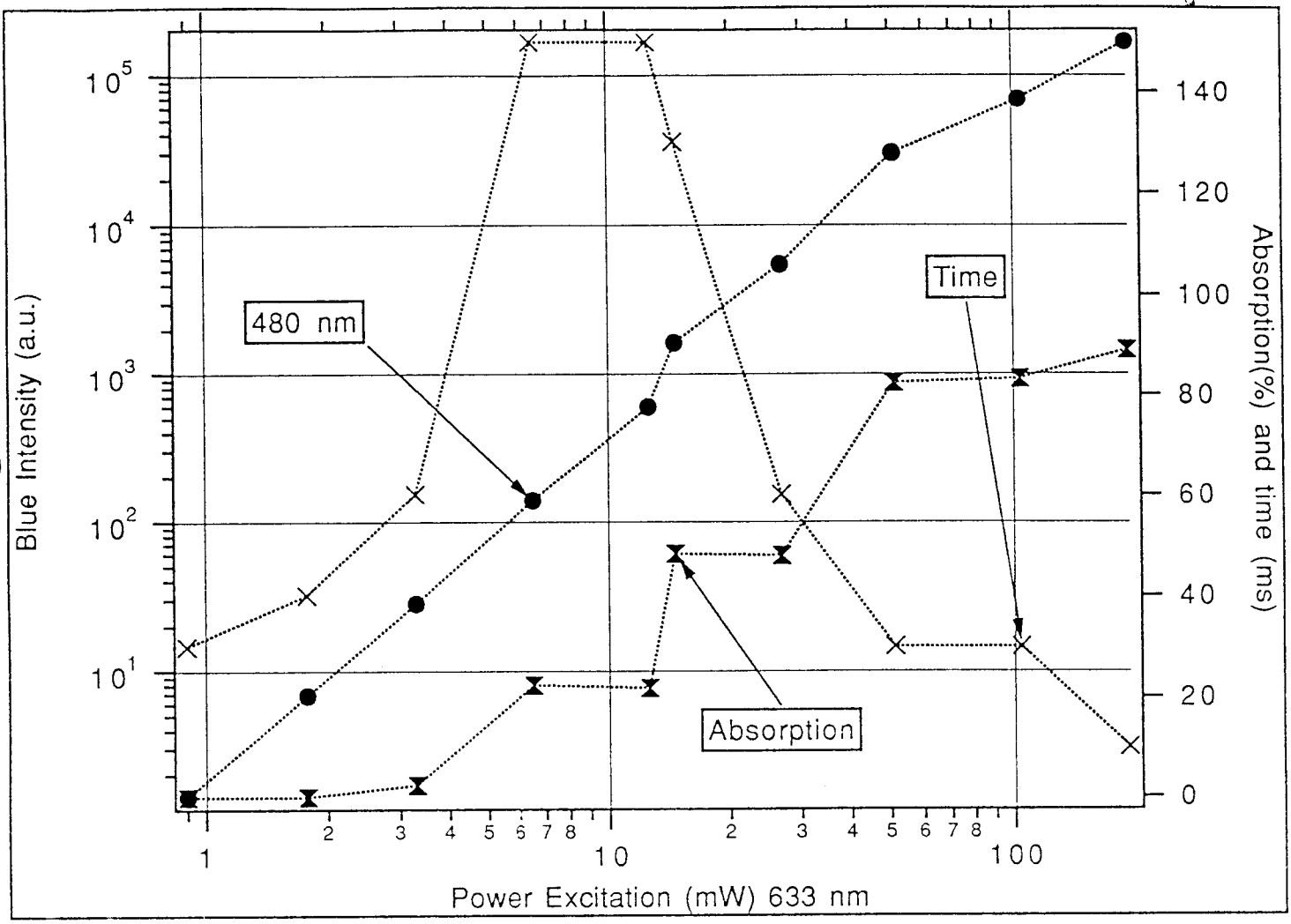
Blue Intensity (a.u.)
Absorption(%) and time (ms)
480 nm
Time
Absorption
Power Excitation (mW) 633 nm

b)

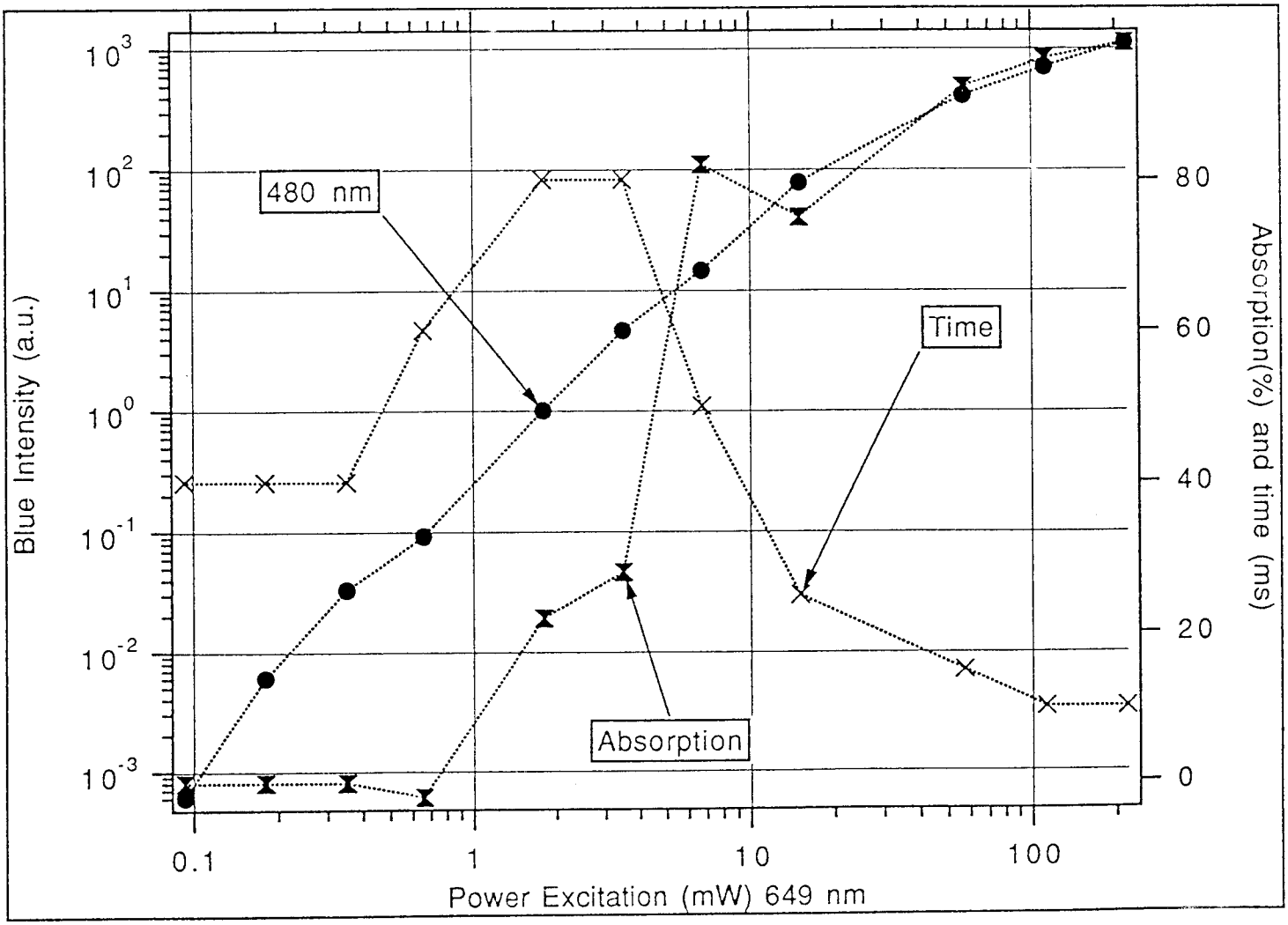
Blue Intensity (a.u.)
Absorption(%) and time (ms)
480 nm
Time
Absorption
Power Excitation (mW) 649 nm

Fig 4

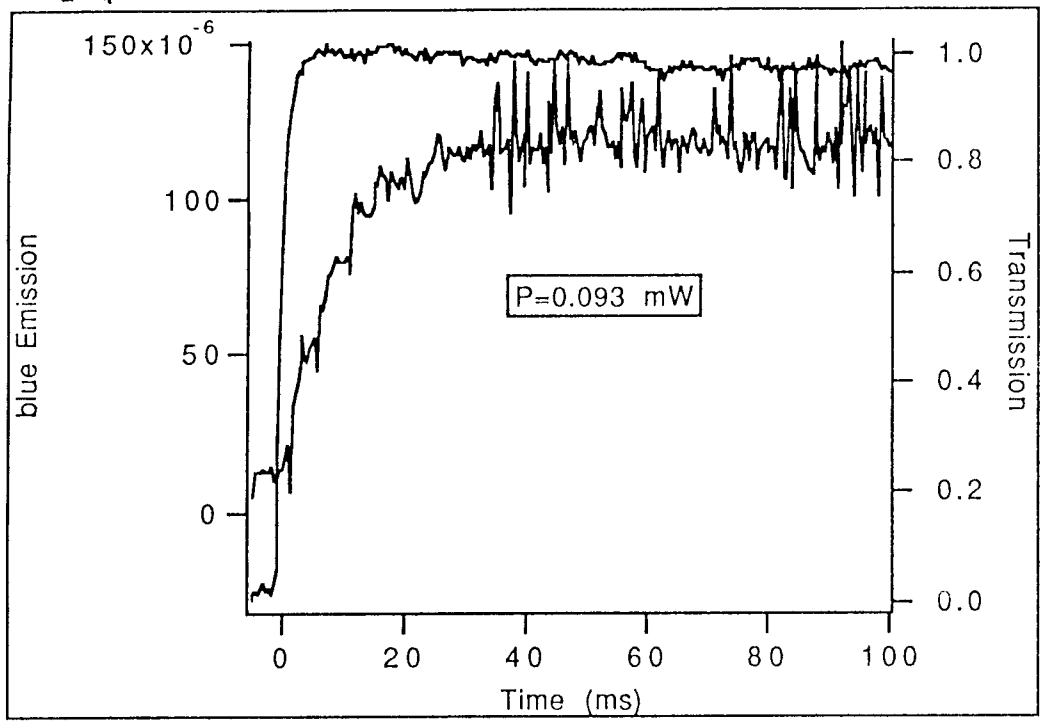
150x10^-6
100
50
0
blue Emission
P=0.093 mW
1.0
0.8
0.6
0.4
0.2
0.0
Transmission
0
20
40
60
80
100
Time (ms)

a

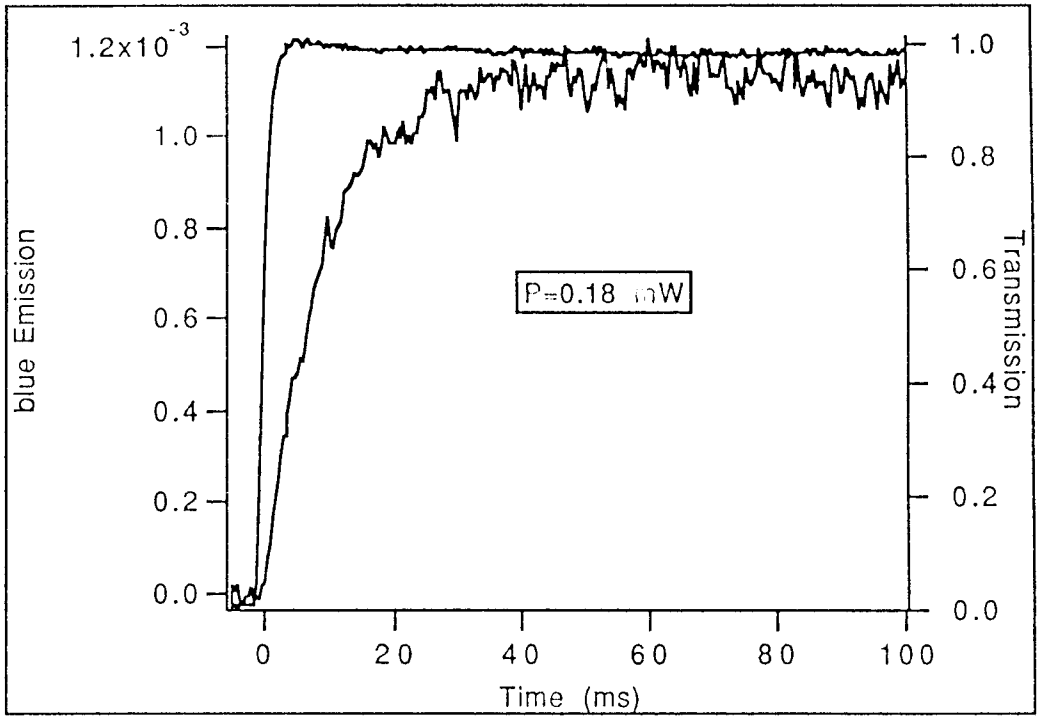
1.2x10^-3
1.0
0.8
0.6
0.4
0.2
0.0
blue Emission
P=0.18 mW
1.0
0.8
0.6
0.4
0.2
0.0
Transmission
0
20
40
60
80
100
Time (ms)

b

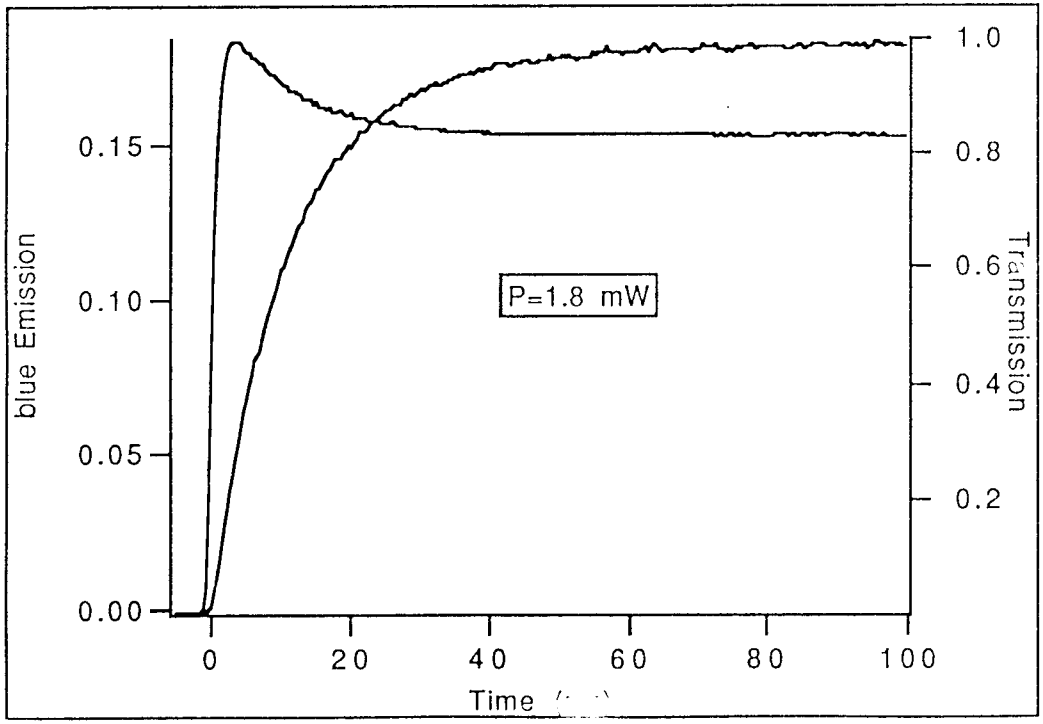
0.15
0.10
0.05
0.00
blue Emission
P=1.8 mW
1.0
0.8
0.6
0.4
0.2
Transmission
0
20
40
60
80
100
Time

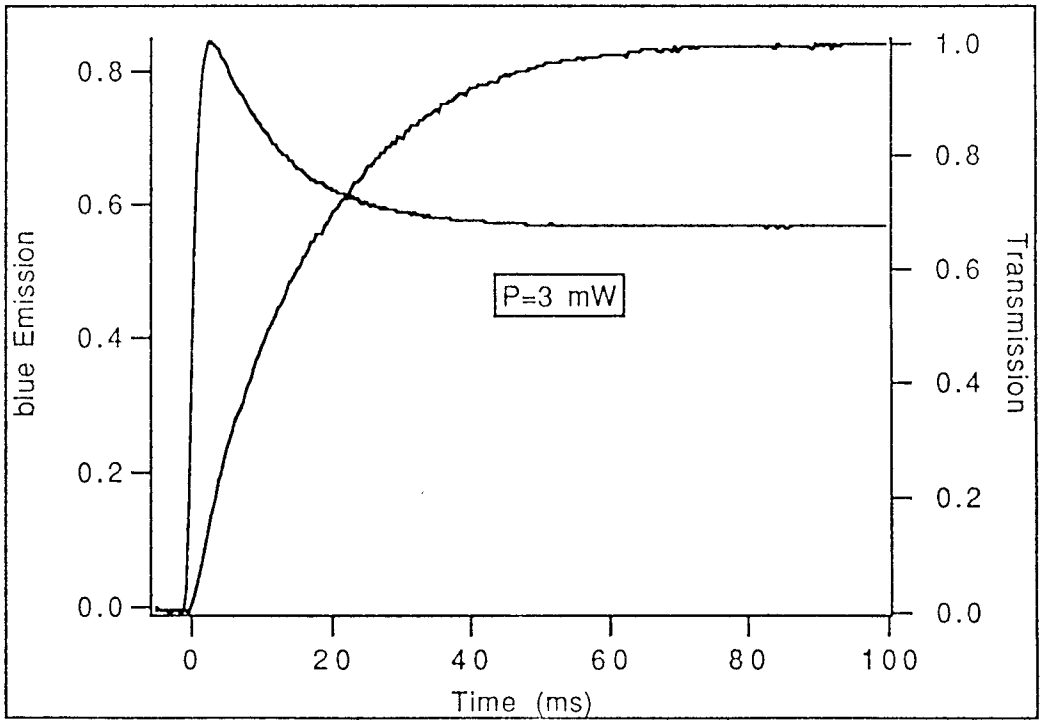
0.8
0.6
0.4
0.2
0.0
blue Emission
P=3 mW
1.0
0.8
0.6
0.4
0.2
0.0
Transmission
0
20
40
60
80
100
Time (ms)

d

Fig 4

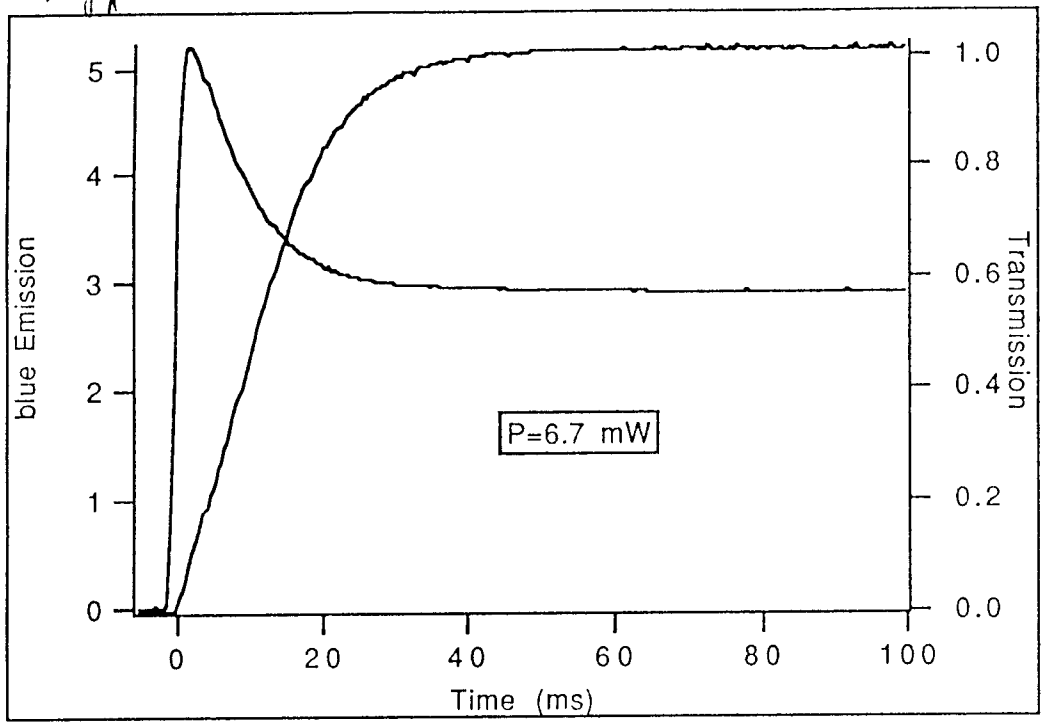
blue Emission
Transmission
P=6.7 mW
Time (ms)

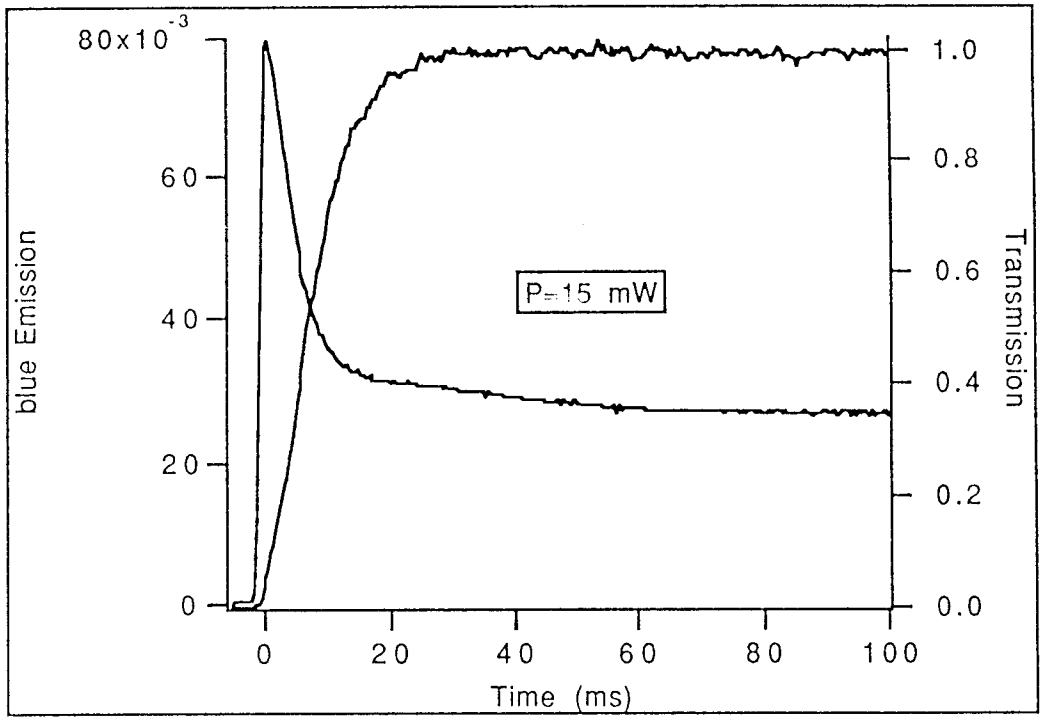
80x10^-3
blue Emission
Transmission
P=15 mW
Time (ms)

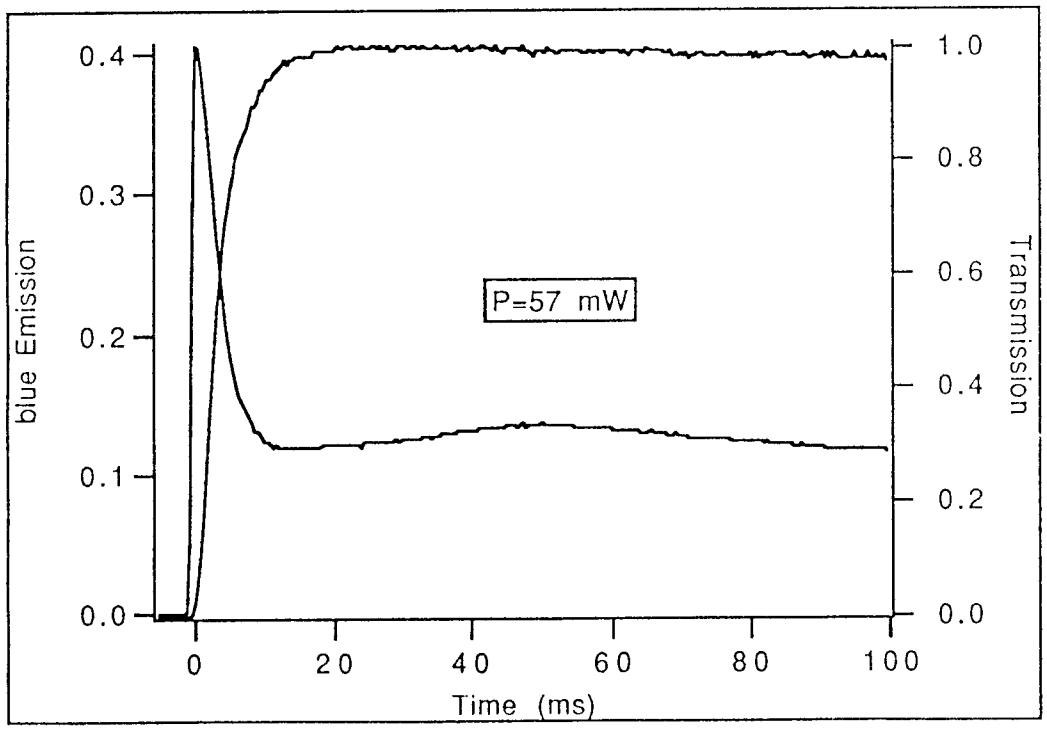
blue Emission
Transmission
P=57 mW
Time (ms)

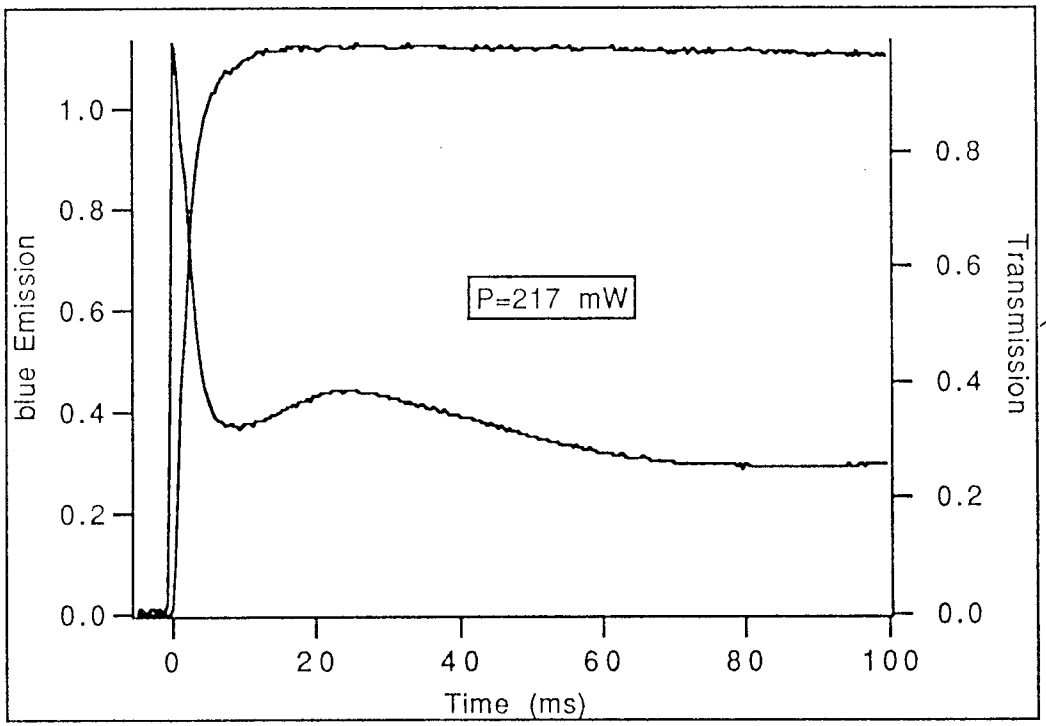
blue Emission
Transmission
P=217 mW
Time (ms)

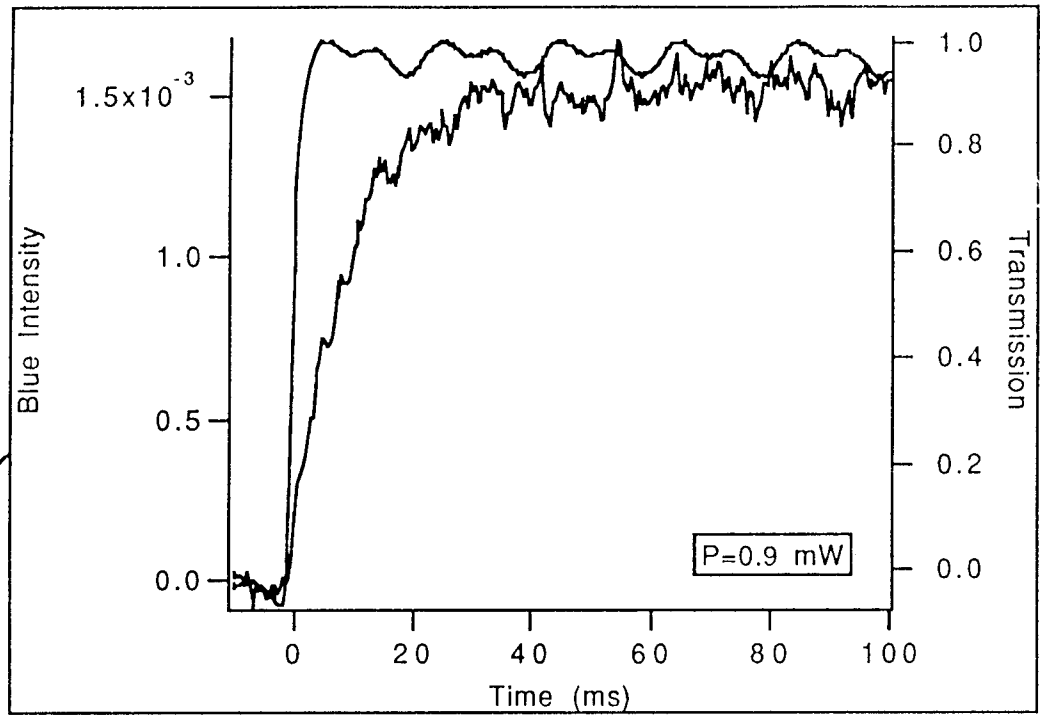
1.5x10^-3
1.0
0.5
0.0
Blue Intensity
1.0
0.8
0.6
0.4
0.2
0.0
Transmission
P=0.9 mW
0
20
40
60
80
100
Time (ms)

a

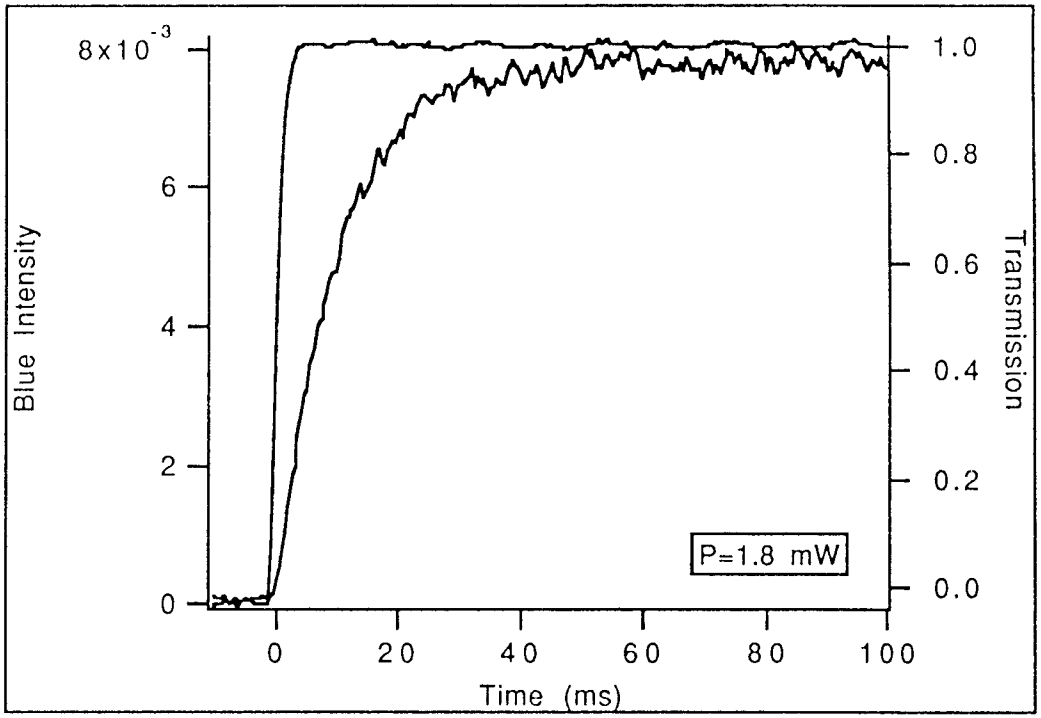
8x10^-3
6
4
2
0
Blue Intensity
1.0
0.8
0.6
0.4
0.2
0.0
Transmission
P=1.8 mW
0
20
40
60
80
100
Time (ms)

b

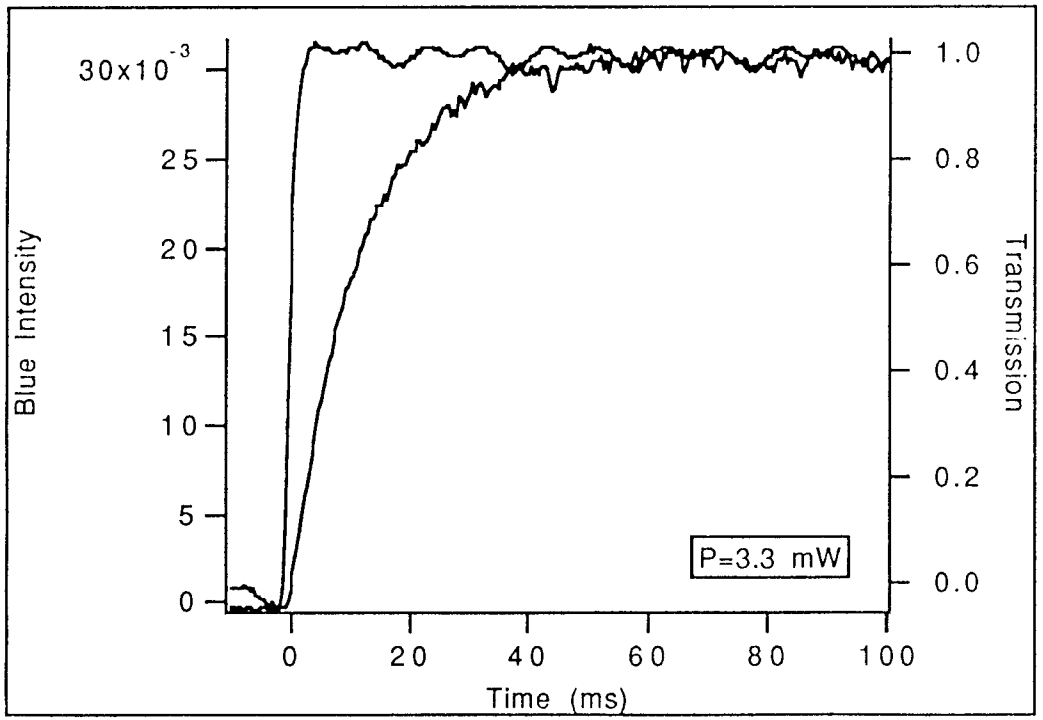
30x10^-3
25
20
15
10
5
0
Blue Intensity
1.0
0.8
0.6
0.4
0.2
0.0
Transmission
P=3.3 mW
0
20
40
60
80
100
Time (ms)

c

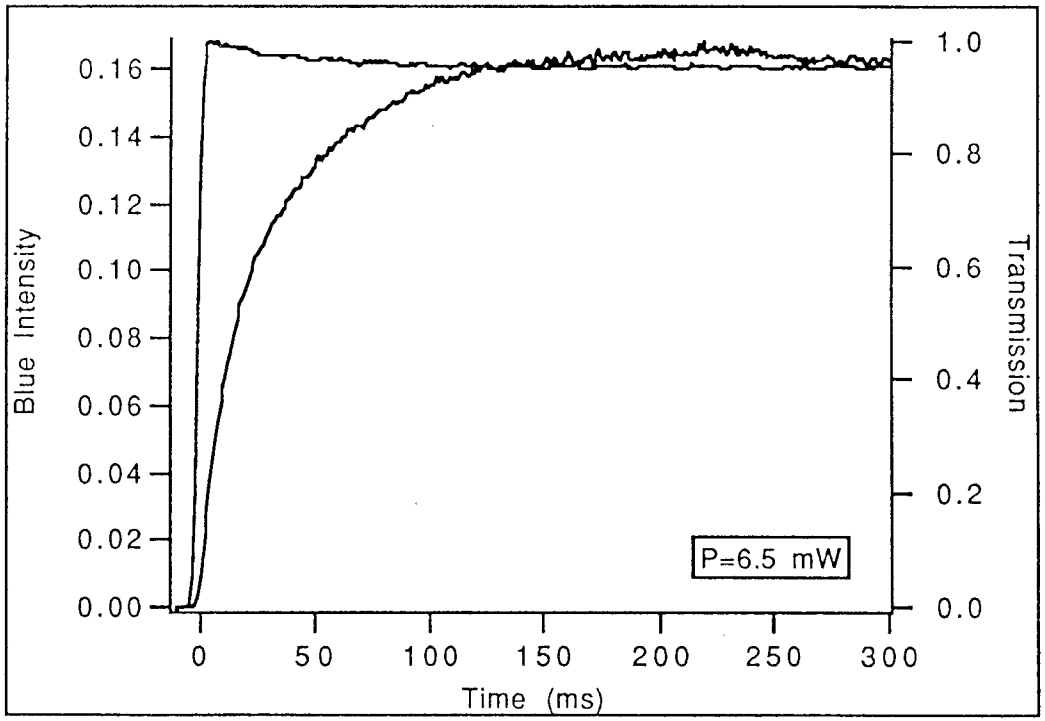
0.16
0.14
0.12
0.10
0.08
0.06
0.04
0.02
0.00
Blue Intensity
1.0
0.8
0.6
0.4
0.2
0.0
Transmission
P=6.5 mW
0
50
100
150
200
250
300
Time (ms)

d

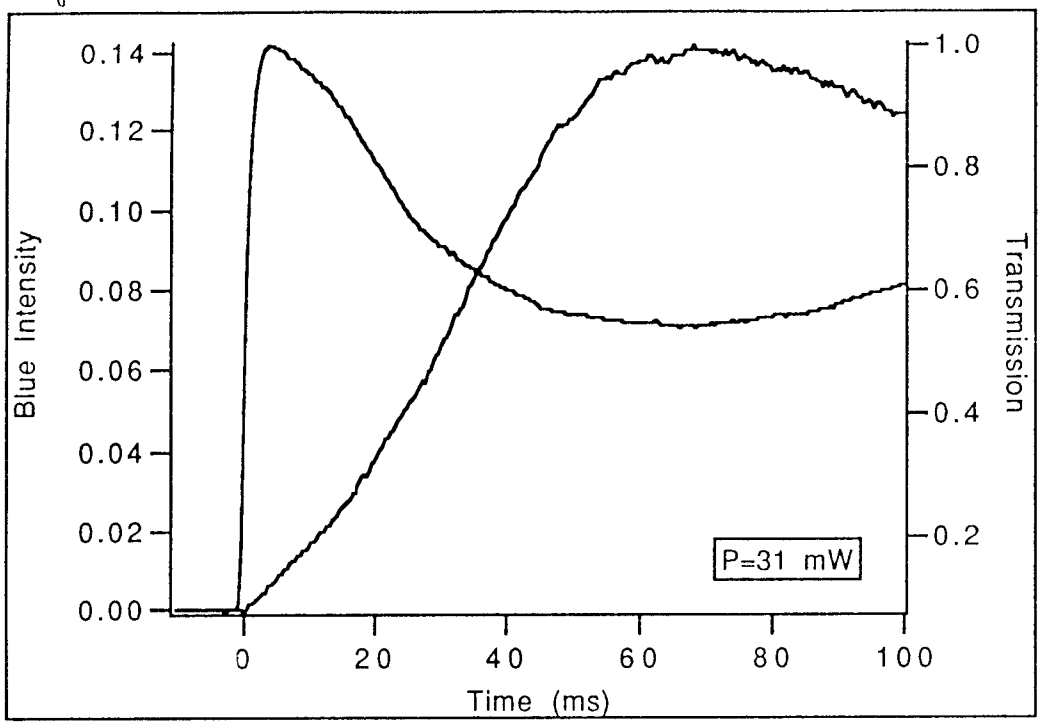
Blue Intensity
Transmission
Time (ms)
P=31 mW

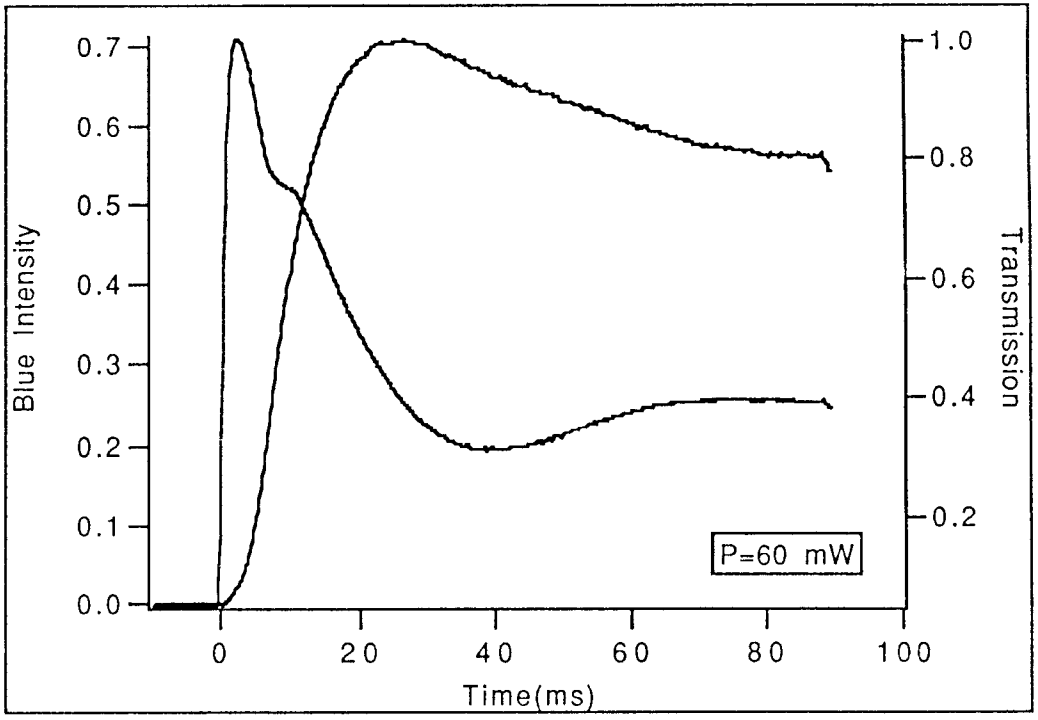
Blue Intensity
Transmission
Time(ms)
P=60 mW

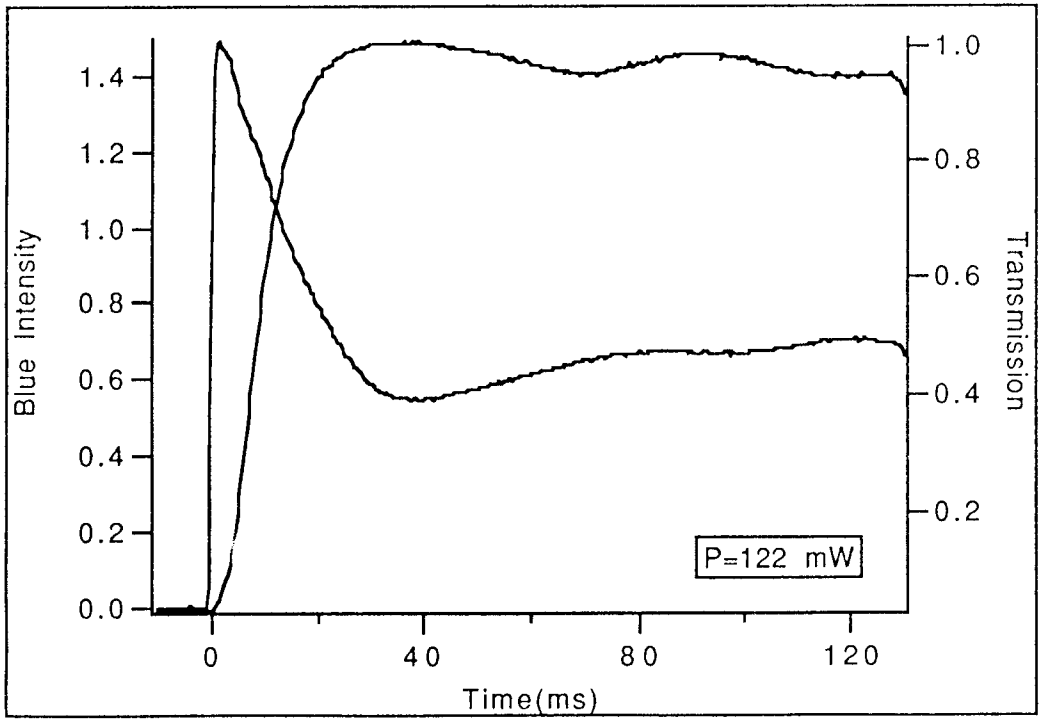
Blue Intensity
Transmission
Time(ms)
P=122 mW

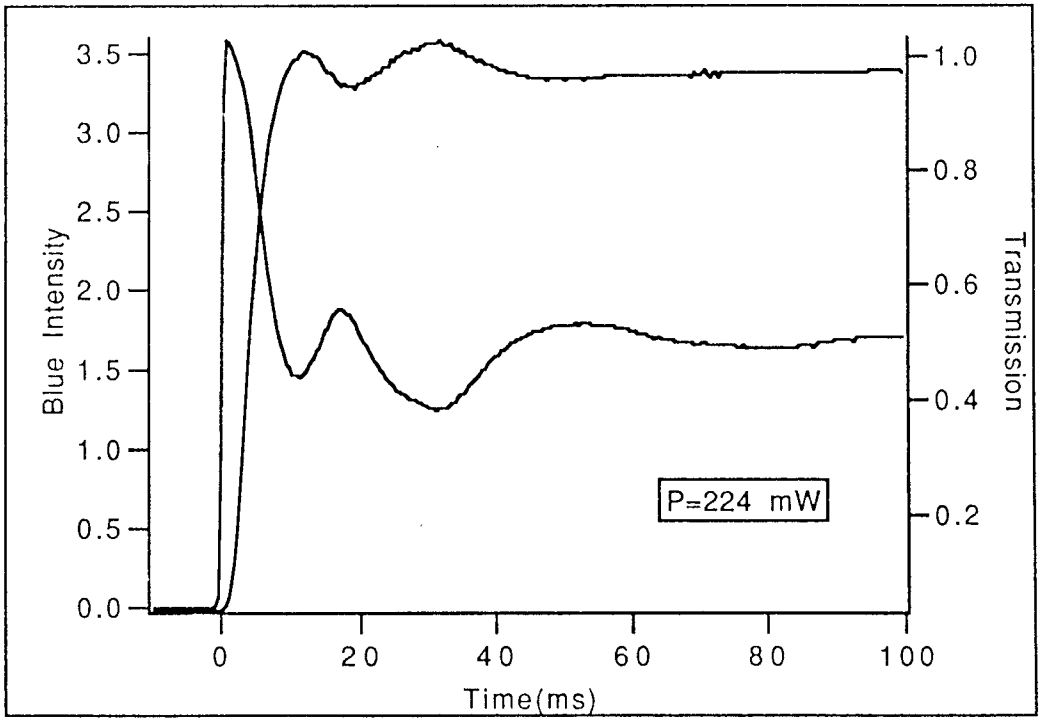
Blue Intensity
Transmission
Time(ms)
P=224 mW

Fig 8

c

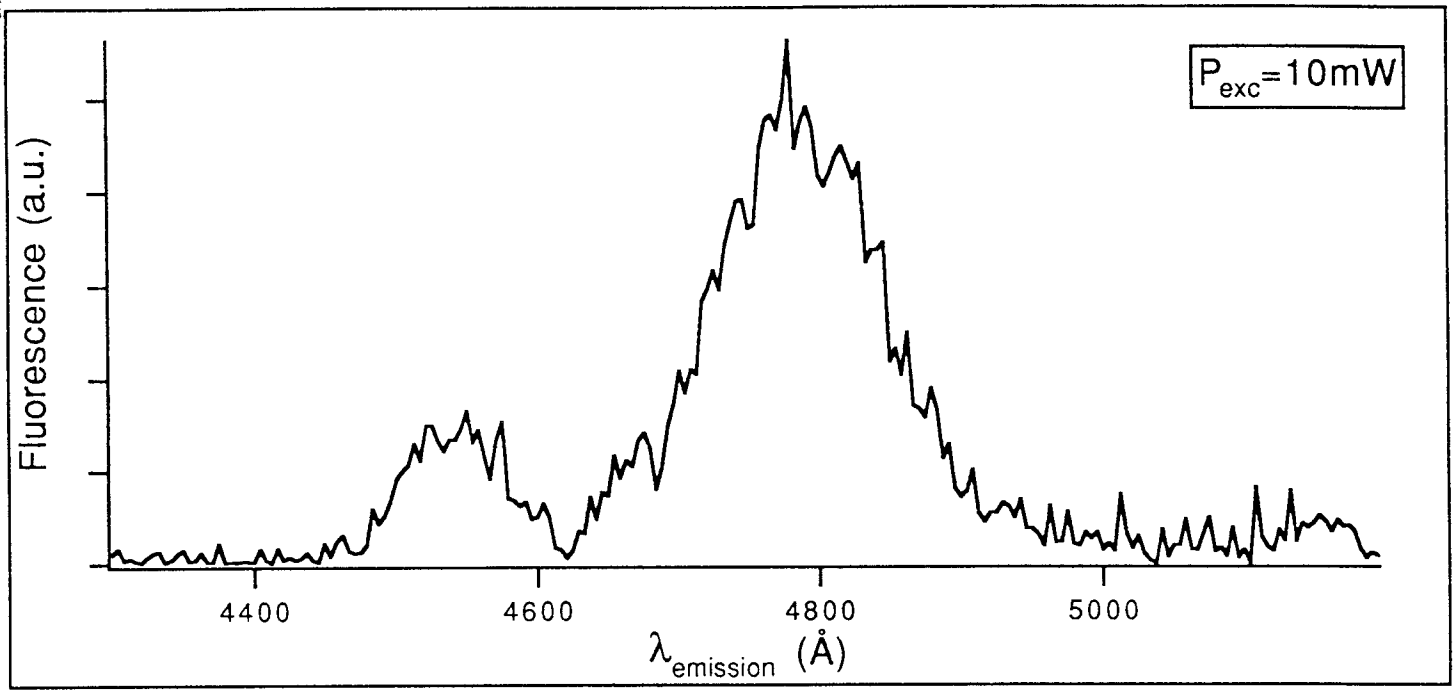
P_{exc}=10mW
Fluorescence (a.u.)
4400
4600
4800
5000
$\lambda_{emission}$ (Å)

b

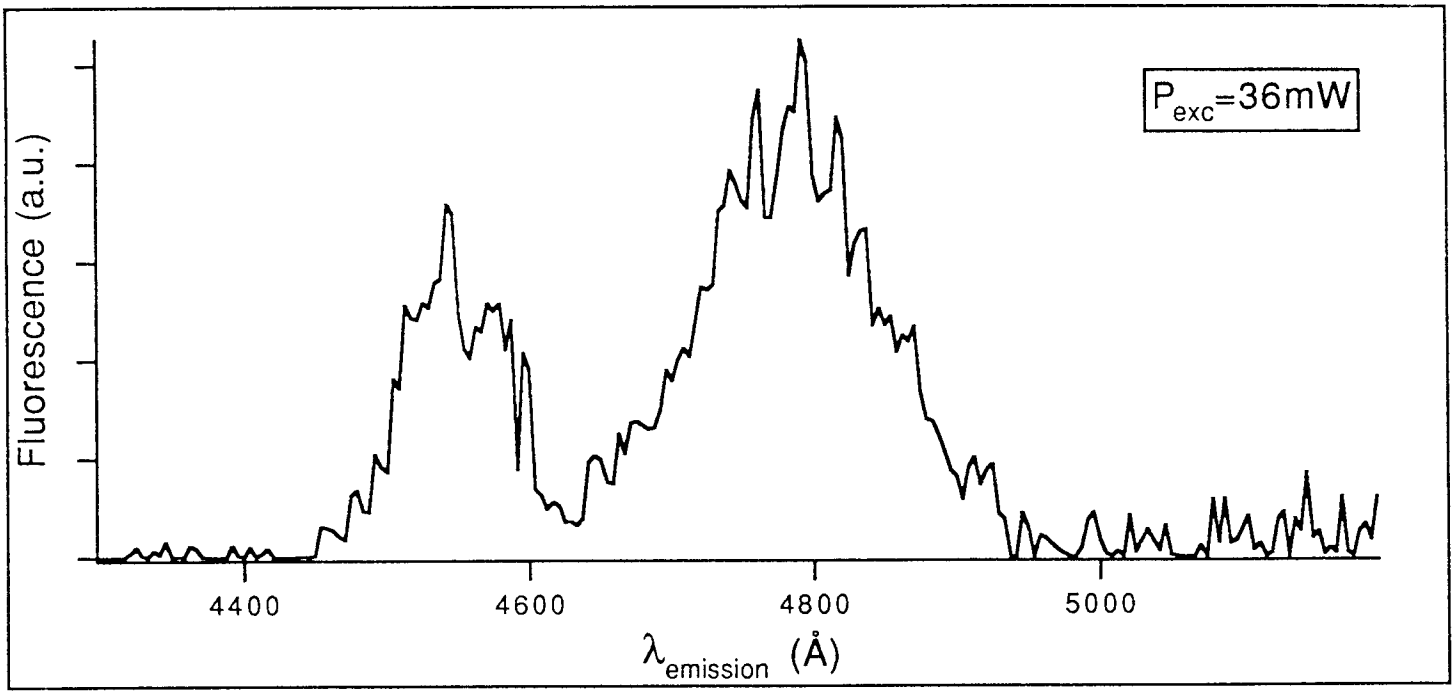
P_{exc}=36mW
Fluorescence (a.u.)
4400
4600
4800
5000
$\lambda_{emission}$ (Å)

a

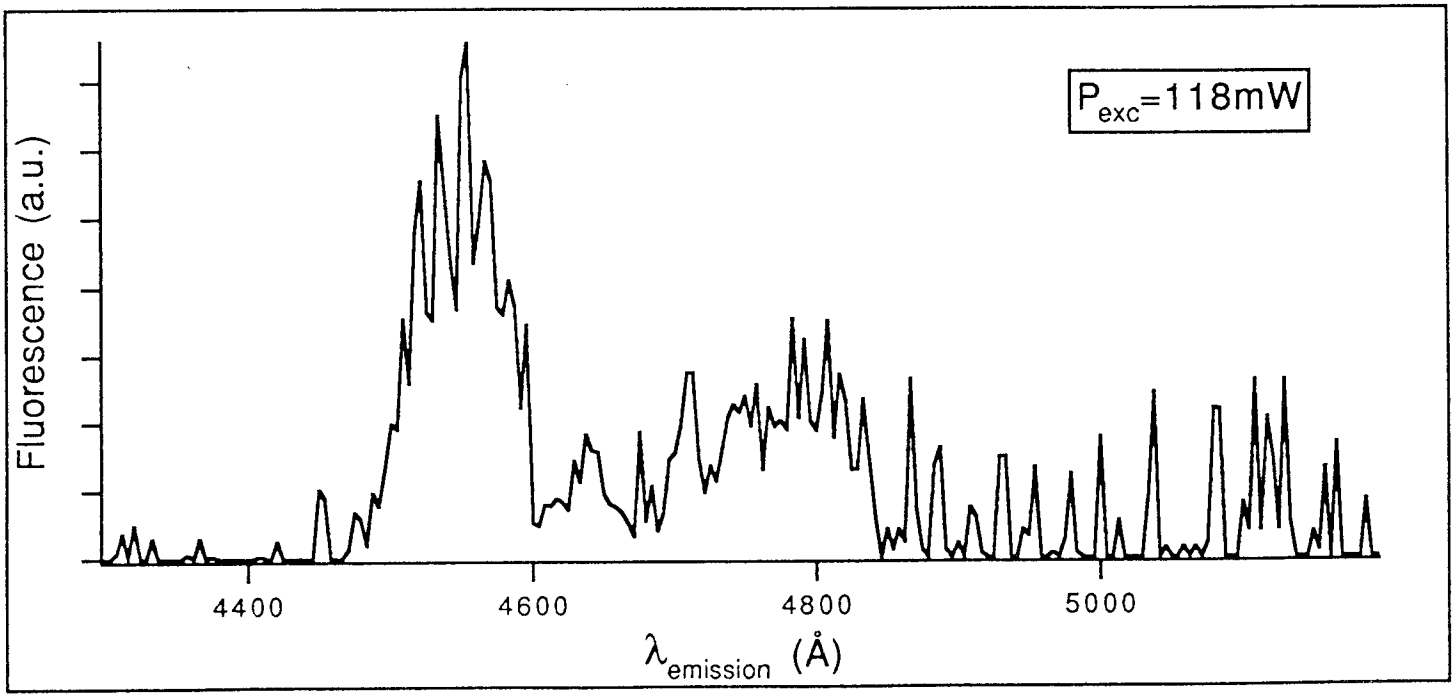
P_{exc}=118mW
Fluorescence (a.u.)
4400
4600
4800
5000
$\lambda_{emission}$ (Å)

b

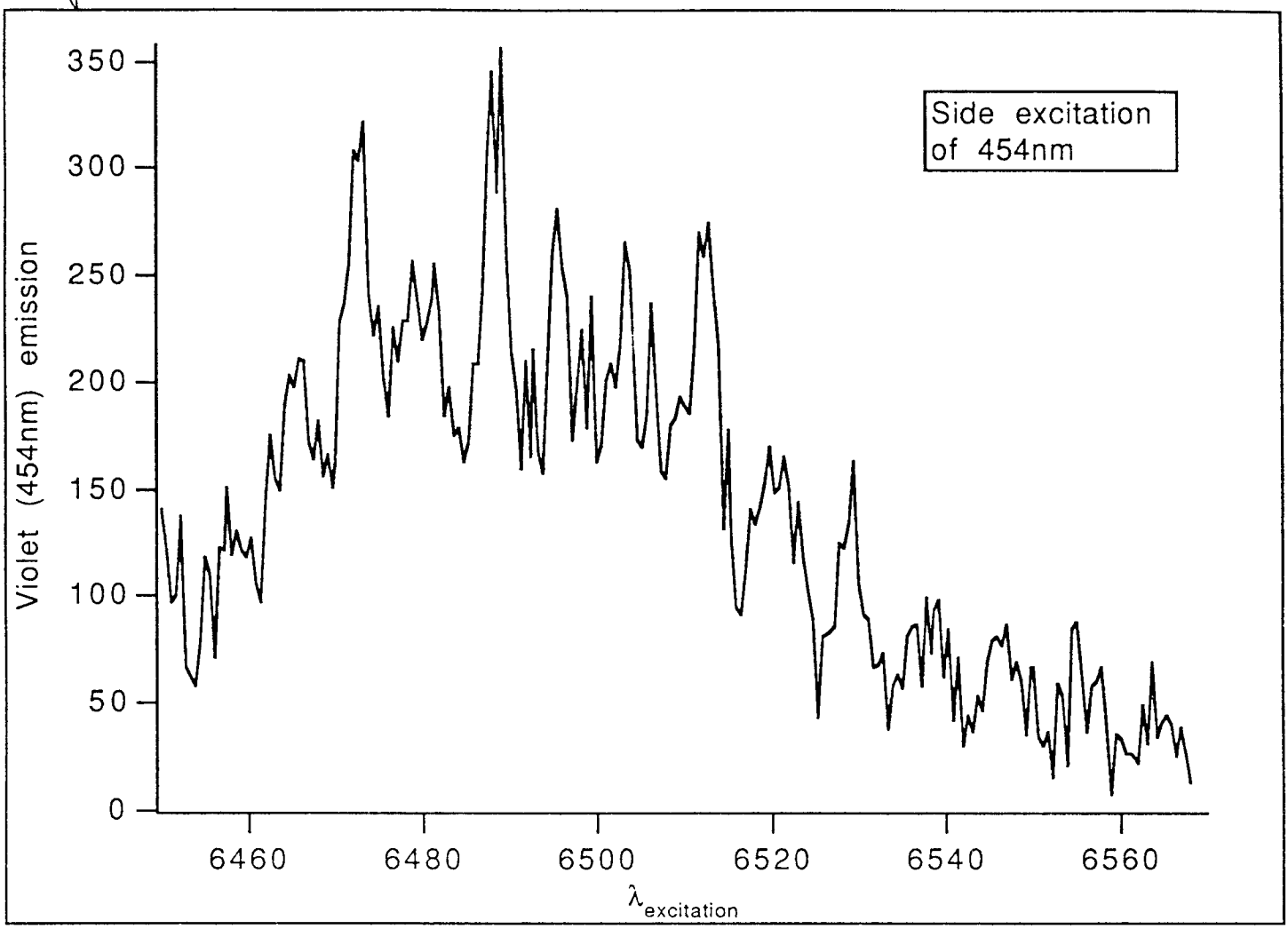
Side excitation
of 454nm
Violet (454nm) emission
350
300
250
200
150
100
50
0
6460
6480
6500
6520
6540
6560
λexcitation

a

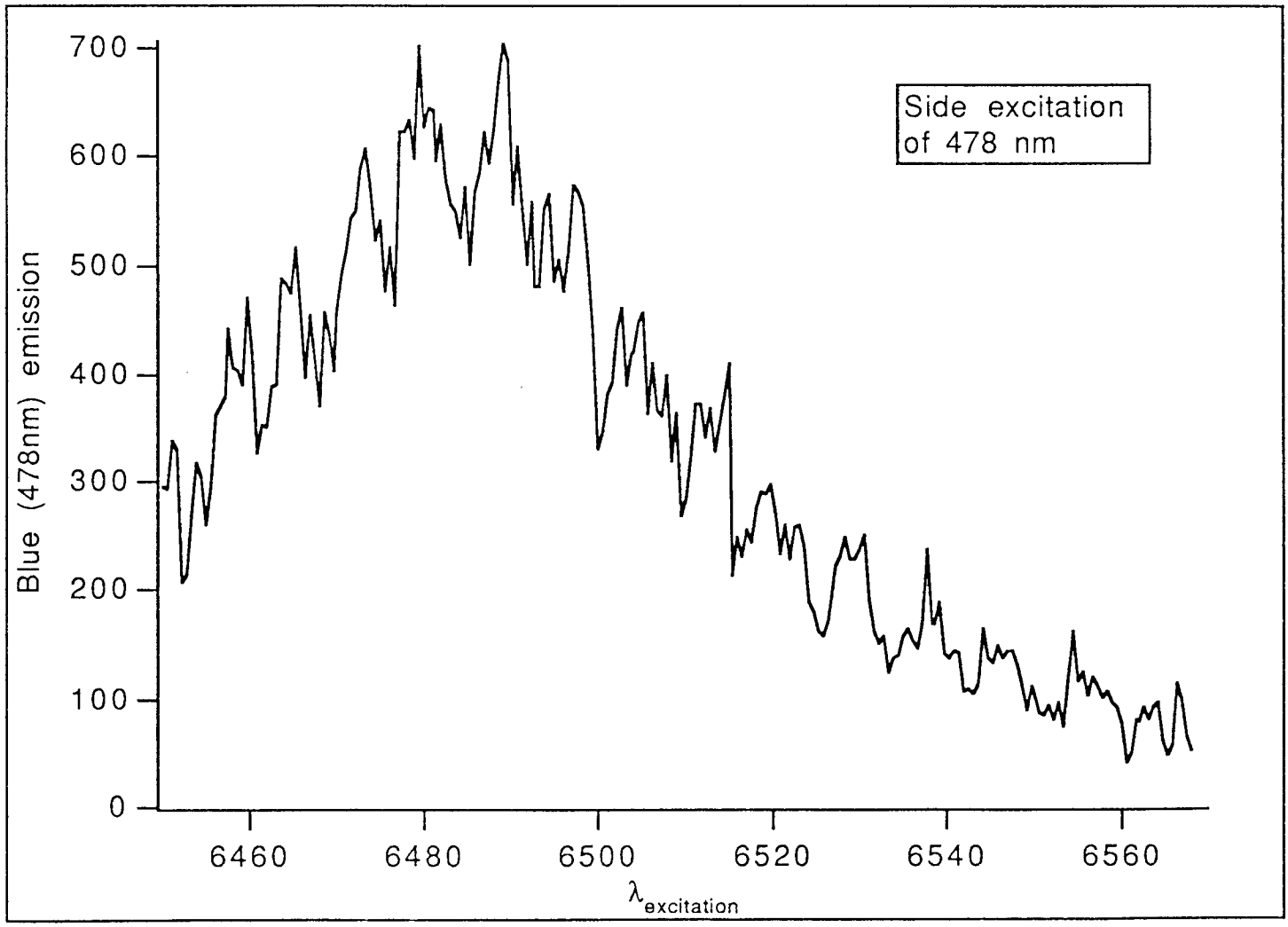
Side excitation
of 478 nm
Blue (478nm) emission
700
600
500
400
300
200
100
0
6460
6480
6500
6520
6540
6560
λexcitation

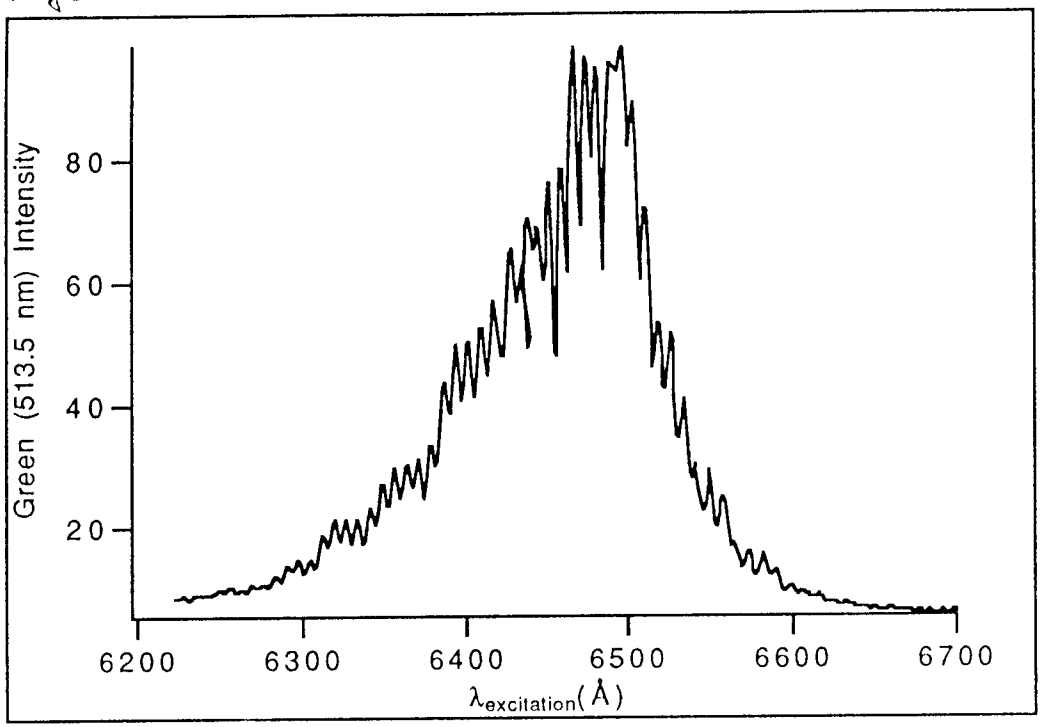
Green (513.5 nm) Intensity
20
40
60
80
6200
6300
6400
6500
6600
6700
λexcitation(Å)

c

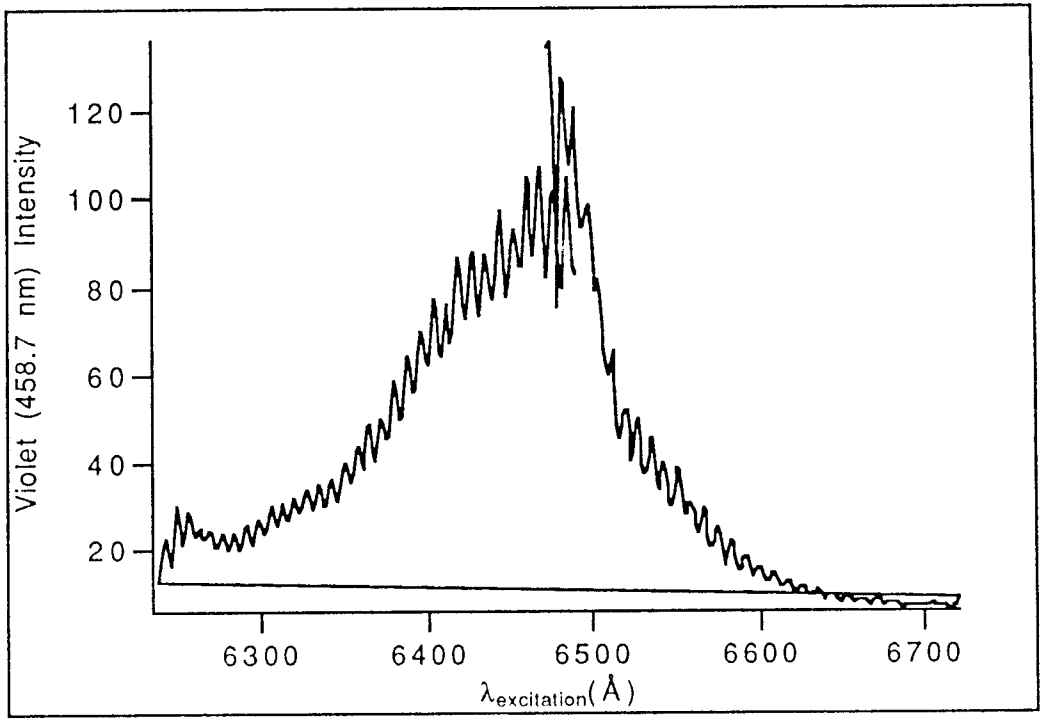
Violet (458.7 nm) Intensity
20
40
60
80
100
120
6300
6400
6500
6600
6700
λexcitation(Å)

b

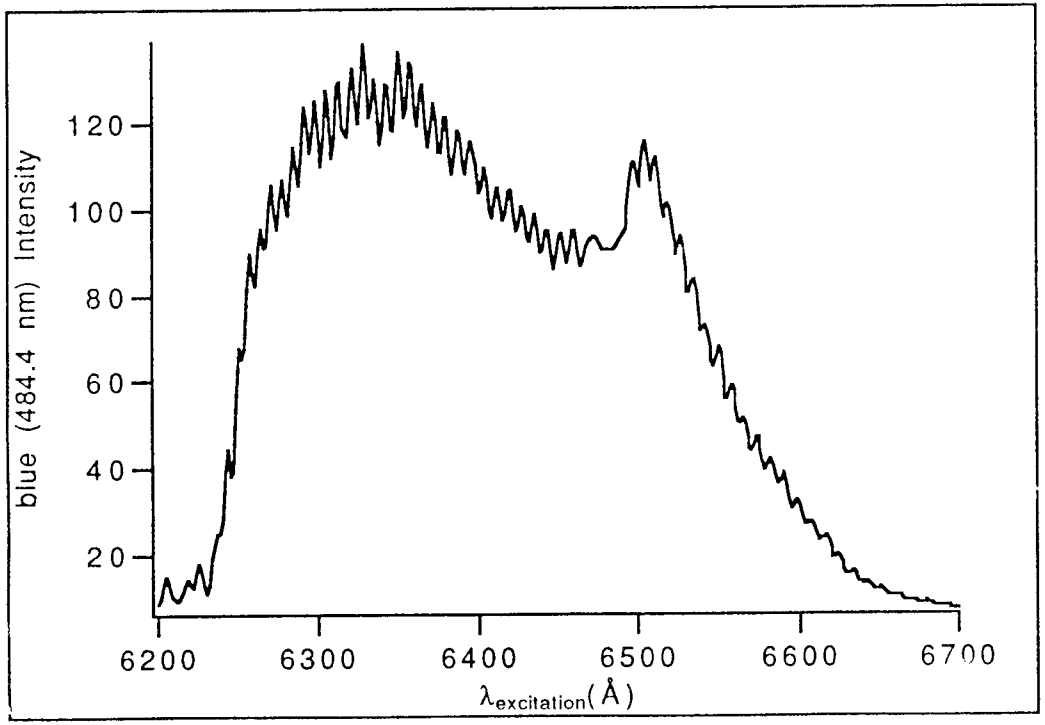
blue (484.4 nm) Intensity
20
40
60
80
100
120
6200
6300
6400
6500
6600
6700
λexcitation(Å)

a

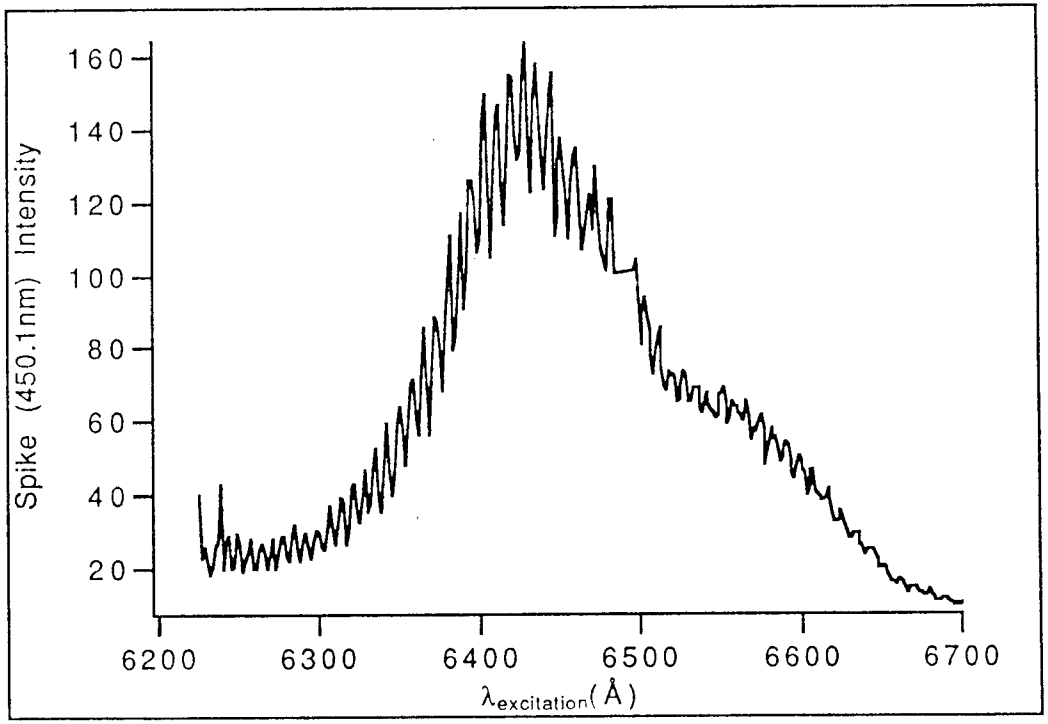
Spike (450.1nm) Intensity
20
40
60
80
100
120
140
160
6200
6300
6400
6500
6600
6700
λexcitation(Å)

d

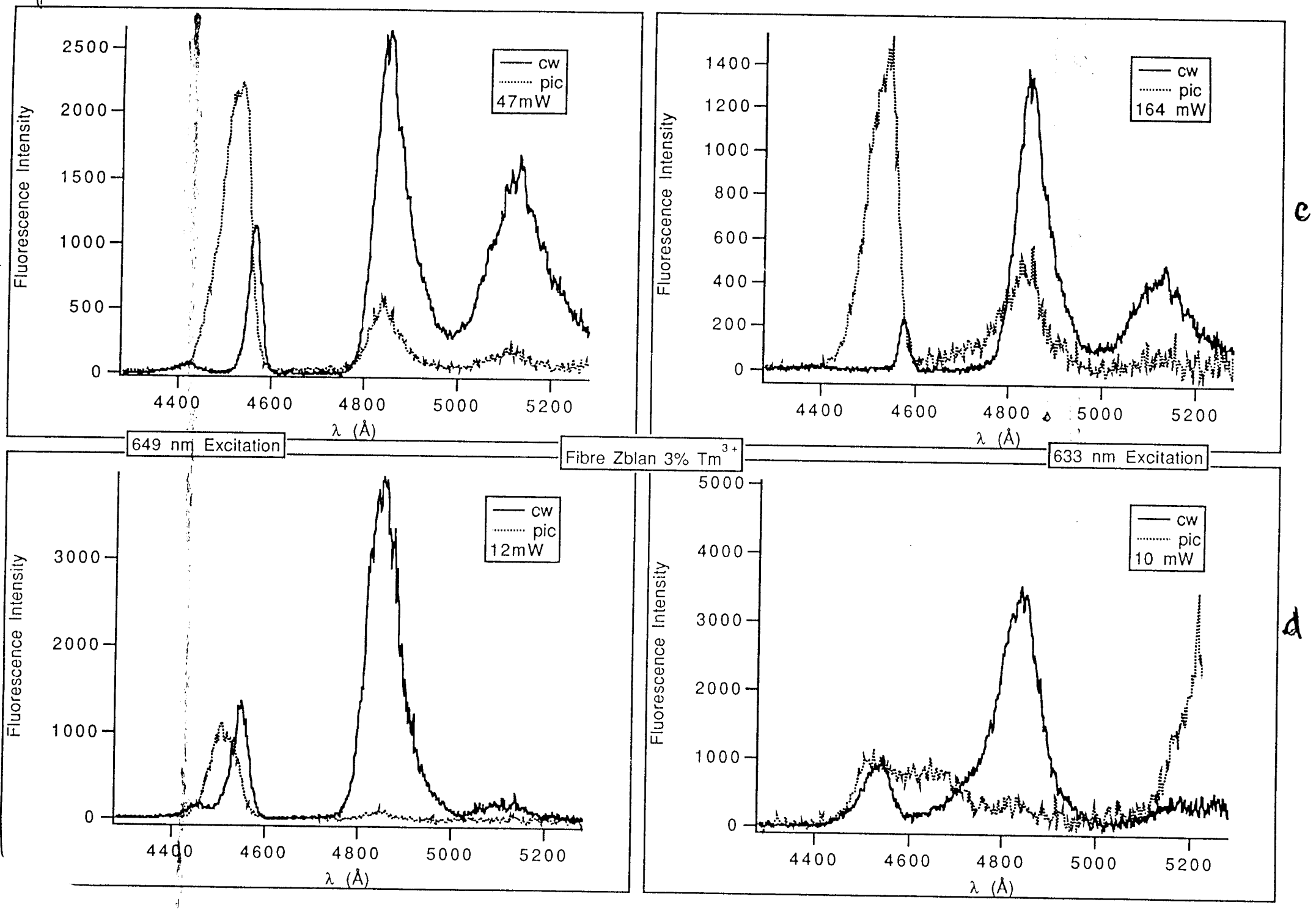
a
Fluorescence Intensity
2500
2000
1500
1000
500
0
4400
4600
4800
5000
5200
λ (Å)
cw
pic
47mW
649 nm Excitation
c
Fluorescence Intensity
1400
1200
1000
800
600
400
200
0
4400
4600
4800
5000
5200
λ (Å)
cw
pic
164 mW
Fibre Zblan 3% Tm 3+
b
Fluorescence Intensity
3000
2000
1000
0
4400
4600
4800
5000
5200
λ (Å)
cw
pic
12mW
633 nm Excitation
d
Fluorescence Intensity
5000
4000
3000
2000
1000
0
4400
4600
4800
5000
5200
λ (Å)
cw
pic
10 mW